Development 123, 143-151
Printed in Great Britain © The Company of Biologists Limited 1996
DEV3463

Mutations affecting morphogenesis during gastrulation and tail formation in the zebrafish, *Danio rerio*

Matthias Hammerschmidt*,†, Francisco Pelegri†, Mary C. Mullins§, Donald A. Kane, Michael Brand¶, Fredericus J. M. van Eeden, Makoto Furutani-Seiki, Michael Granato, Pascal Haffter, Carl-Philipp Heisenberg, Yun-Jin Jiang, Robert N. Kelsh‡, Jörg Odenthal, Rachel M. Warga and Christiane Nüsslein-Volhard

Max-Planck-Institut für Entwicklungsbiologie, Abteilung für Genetik, Spemannstraße 35/III, 72076 Tübingen, Germany

*Author for correspondence at present address: Harvard University, Department of Molecular and Cellular Biology, 16 Divinity Avenue, Cambridge, MA 02138, USA (e-mail: mhammer@hubio2.harvard.edu)
†M. H. and F. P. contributed equally to this work
‡Present address: Institute of Neuroscience, University of Oregon, Eugene, OR 97405, USA
§Present address: University of Pennsylvania, Department of Cell and Developmental Biology, 605 Stellar-Chance, Philadelphia, PA 19104-6058, USA
¶Present address: Institut für Neurobiologie, Universität Heidelberg, Im Neuenheimer Feld 364, 69120 Heidelberg, Germany

SUMMARY

We have identified several genes that are required for various morphogenetic processes during gastrulation and tail formation. Two genes are required in the anterior region of the body axis: *one eyed pinhead* (*oep*) and *dirty nose* (*dns*). *oep* mutant embryos are defective in prechordal plate formation and the specification of anterior and ventral structures of the central nervous system. In *dns* mutants, cells of the prechordal plate, such as the prospective hatching gland cells, fail to specify.

Two genes are required for convergence and extension movements. In mutant *trilobite* embryos, extension movements on the dorsal side of the embryo are affected, whereas in the formerly described *spadetail* mutants, for which two new alleles have been isolated, convergent movements of ventrolateral cells to the dorsal side are blocked.

Two genes are required for the development of the posterior end of the body axis. In *pipetail* mutants, the tailbud fails to move ventrally on the yolk sac after germ ring closure, and the tip of the tail fails to detach from the yolk tube. Mutants in *kugelig* (*kgg*) do not form the yolk tube at the posterior side of the yolk sac.

Key words: zebrafish, gastrulation, tail formation, axis extension, cyclopia, *one-eyed-pinhead, spadetail, trilobite, pipetail, kugelig*

INTRODUCTION

Rapid progress has been made in the understanding of the cellular behavior underlying the morphogenetic movements during vertebrate gastrulation and tail formation. In gastrulating zebrafish embryos, three morphogenetic movements can be distinguished: epiboly, involution and dorsal convergent extension, which are driven by radial and medial cell intercalation and active cell migration (Warga and Kimmel, 1990).

However, very little is known about the genes controlling these movements. Treatment of pregastrula embryos with α-amanitin blocks all gastrulation movement, indicating that they depend on zygotic gene expression (Kane et al., 1996). In zebrafish, two mutants with defects in gastrulation movements have been described: *spadetail* mutant embryos lack the trunk somites and have a greatly enlarged tail (Kimmel et al., 1989). These defects are caused by a reduction of dorsal convergence movements (Ho and Kane, 1990). *cyclops* mutant embryos (Hatta et al., 1991) exhibit a fusion of the eyes and a lack of ventral specification within the neuroectoderm. The anterior defects might be caused by defects in cell migration of the anterior dorsal mesendodermal cells (Thisse et al., 1994).

Among the cloned genes that are expressed during gastrulation, only a few have been shown to be involved in gastrulation movements. Studies in *Xenopus* animal cap explants have shown that maternal factors that induce mesoderm simultaneously initiate convergent extension movements, suggesting that the early processes of pattern formation and gastrulation may be coupled and share elements of the same genetic control system (Smith and Howard, 1992). This control system might also include genes that are zygotically expressed during gastrulation: *goosecoid*, a homeobox gene expressed in the anterior dorsal mesoderm, seems to play a role in the migration of anterior dorsal mesodermal cells to their final destination in the head region (Niehrs et al., 1993).

According to recent studies in *Xenopus*, tail formation is a continuation of gastrulation and shares components of the same control system that is used in the trunk (Gont et al., 1993; Tucker and Slack, 1995). Cell-labeling studies indicate that cells in the tailbud, the organizer of the tail, derive from cells of the blastopore lip, the organizer of the trunk. Moreover, the cellular movements in the tail resemble those in the blastopore. The tight linkage of gastrulation and tail formation is also revealed by the phenotypes of ventralized and dorsalized

zebrafish mutants: in all mutants isolated, the dorsoventral patterning of both trunk and tail are affected (Hammerschmidt et al., 1996; Mullins et al., 1996). However, additional morphogenetic processes are initiated after gastrulation that appear to be uniquely required for the posterior extension of the body axis and the outgrowth of the tail. In the zebrafish, these are the ventral movement of the tailbud on the yolk sac, the constriction of the posterior part of the yolk sac to form the yolk tube, and the detachment of the tip of the tail from the yolk tube. Therefore, there could be genes that are uniquely required for specific aspects of zebrafish tail development.

Here, we describe the isolation of zebrafish mutants that show specific defects during gastrulation and tail formation. *one-eyed pinhead* mutants display defects in the specification of the prechordal plate, which lead to an impaired rostral outgrowth of the body axis, while in *spadetail* and *trilobite* mutants, convergent and extension movements are affected. *pipetail* and *kugelig* mutants display specific defects during tail formation.

MATERIALS AND METHODS

Fish maintenance and photography

Mutations were induced and zebrafish maintained, mated and raised as previously described (Mullins et al., 1994). Embryos were kept at 28°C and staged according to Kimmel et al. (1995). For photography, embryos were dechorionated and mounted in 5% methylcellulose in E3 medium (Westerfield, 1994). Older embryos were anesthetized with 1/10 volume of 0.2% MESAB (Sigma).

In situ hybridization and immunostaining

Immunostainings were carried out as described elsewhere (Schulte-Merker et al., 1992) with slight modifications: the blocking, but not the incubation solution, was supplemented with 100 μM biotin; the incubation solution of the secondary antibody was supplemented with 1% normal goat serum (Vector); and the secondary antibody was preincubated for 2 hours with zebrafish embryos.

In situ hybridization was carried out as described elsewhere (Schulte-Merker et al., 1992) with the following modifications: hybridization and all washes were carried out at 65°C. Washes were as follows: 1× 20 minutes in 5× SSCT, 50% formamide; 2× 20 minutes in 2× SSCT, 50% formamide; 1× 10 minutes in 2× SSCT, 25% formamide, 1× 10 minutes in 2× SSCT, 2× 30 minutes in 0.2× SSCT, 1× 10 minutes in PBST. Stained embryos were fixed for 2-6 hours at room temperature in 4% paraformaldehyde/PBS, transferred to methanol and stored at 4°C in benzylbenzoate:benzylalcohol (2:1, v:v).

RESULTS

In our screen for mutants affected in morphogenesis and pattern formation during zebrafish embryogenesis, a number of mutants were isolated that show abnormalities in gastrulation and tail formation. In complementation tests, at least 18 genes were identified. At least seven of them are required for the establishment of the basic body plan, and mutant embryos display partial dorsalization (five genes, Mullins et al., 1996) or ventralization (two genes, Hammerschmidt et al., 1996). A number of genes with unique phenotypes affect specific aspects of early processes, such as epiboly (Kane et al., 1996). Here, we describe genes required for other morphogenetic processes during gastrulation and tail formation (*one eyed pinhead*, *dirty nose*, *trilobite*, *spadetail*, *pipetail*, *kugelig* and others; see Table 1). Additional mutants affecting gastrulation are *silberblick* (Heisenberg et al., 1996) and *cyclops* (Brand et al., 1996).

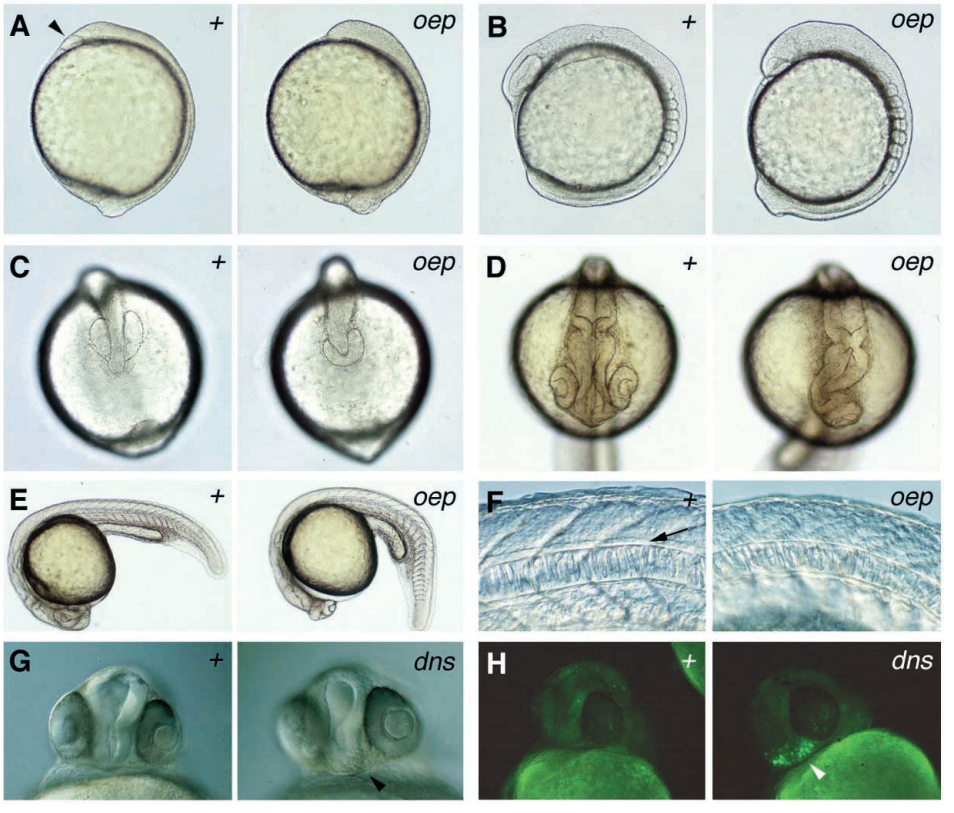

Fig. 1. Morphological characteristics of (A-F) *one-eyed pinhead* (*oep*^{tz257}) and (G,H) *dirty nose* (*dns*^{te350}) mutant embryos. In each section, wild type (+) is to the left, mutant to the right. (A) Tailbud stage, lateral view: the body axis is shorter; no pillow (indicated by an arrowhead) is formed at the anterior end of the hypoblast. (B,C) 8-somite stage: (B) lateral view, the head is reduced while the tailbud seems enlarged in *oep* mutants. (C) dorsal view of head region. (D) 24 hours, dorsal view of head region: the anterior part of the forebrain is missing while the eye vesicles are fused in *oep* mutants. (E) 24 hours, lateral view: the notochord is slightly undulated, the somites are slightly expanded along the a/p axis, the yolk tube is shorter and thicker, and the tail is curled down in *oep* mutants. (F) 24 hours, lateral view at level of yolk tube: no floorplate (arrow) can be detected in *oep* mutants. (G,H) *dns*, 24 hours, ventral view of head region: (G) brownish cells can be observed underneath the eyes (arrowhead); (H) acridine orange staining reveals apoptotic cells in the same region (arrowhead).

Morphology of *one-eyed pinhead* mutants

One allele of *one-eyed pinhead*, *oep*^{tz257}, was isolated, and two more alleles were found in other laboratories (Schier et al., 1996; U. Strähle, S. Jesuthasan, P. Blader, P. Garcia-Villalba, K. Hatta and P. W. Ingham, personal communication). Morphologically, the phenotype of *oep* mutants is recognizable at the tailbud stage (Fig. 1A): the body axis is shorter, the head region is thicker and no prechordal plate can be found. Despite the lack of the anterior structures, no increase in the rate of cell death could be detected in the anterior region at gastrula and somite stages by acridine orange stainings (not shown). The notochord, the somites, and other structures in the posterior trunk develop normally during early somite stages (Fig. 1B), although the tailbud is more prominent in *oep* mutants (Fig. 1B). A dorsal view on the head region reveals that the anterior part of the forebrain is reduced, while the eye vesicles are fused (Fig. 1C); brain structures posterior to the forebrain are normally formed (Fig. 1D). In the trunk (Figs 1E, 2K), the notochord is slightly undulated, and the yolk tube is smaller and thicker, suggesting that the extension of the body axis is impaired. The body axis is curled down, and no floorplate cells can be morphologically detected (Fig. 1F). The hatching gland, a derivative of the prechordal plate, is not formed.

Altered mesodermal and neuroectodermal gene expression before and during gastrulation of *oep* mutants

With molecular markers, alterations are first visible in the presumptive dorsal mesoderm, where the expression of *goosecoid* (*gsc*; Stachel et al., 1993; Schulte-Merker et al., 1994; Thisse et al., 1994) is progressively reduced, beginning before gastrulation, as shown here at 40% epiboly (Fig. 2A). At 70% epiboly, no *gsc* transcripts have been detected in most *oep* mutant embryos, while a few show some residual *gsc* staining. In those embryos, the *gsc* expression domain lacks the arrowhead-like anterior protrusion found in wild-type siblings (not shown), suggesting that in the mutants, the cells with the reduced *gsc* expression fail to move normally towards and beyond the animal pole. The lack of the prechordal plate is also revealed by the absence of its derivatives, the hatching gland precursors, which are marked by the expression of the forkhead domain gene *fkd2* (R.M.W. and J.O., unpublished). At the 10-somite stage, no or only very few *fkd2*-positive cells (up to 10 versus about 200 in wild type) are present anterior of the head region (Fig. 2D).

In contrast to the prechordal plate, the axial mesoderm of the trunk, the notochord anlage, appears normal during gas-

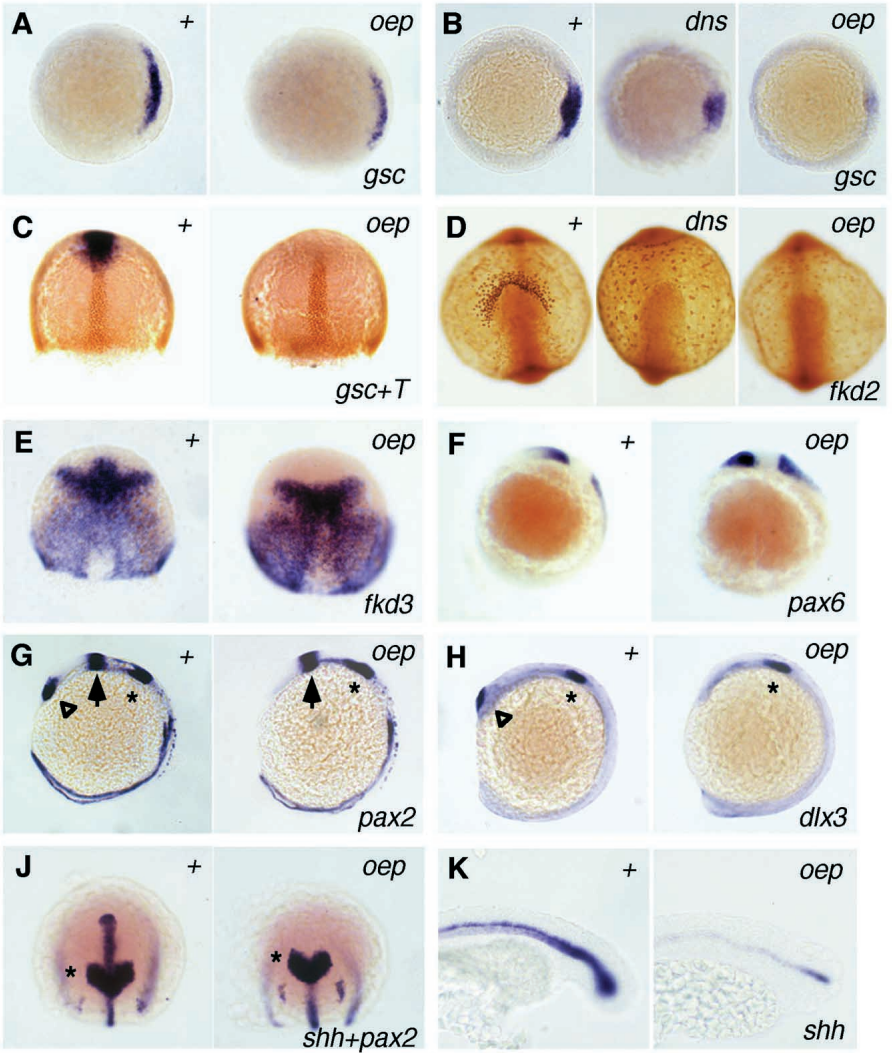

Fig. 2. Altered gene expression in mesoderm and neuroectoderm of *oep* and *dns* mutants revealed by in situ hybridization (A-C, E-K) and immunostaining (C,D). In each section, wild type (+) is to the left, mutants to the right. (A) *gsc*, 40% epiboly, animal view, dorsal right. (B) *gsc*, shield, animal view, dorsal right. (C) *gsc* mRNA in blue and Ntl protein (T) in brown, 70% epiboly, dorsal view. (D) *fkd2*, 10-somite stage, view on head: *fkd2*-positive presumptive hatching gland cells are absent in *oep* mutants. In *dns* mutants, very small *fkd2*-positive cells can be found at the anterior border of the hypoblast rather than in adjacent regions of the yolk sac. (E) *fkd3*, 70% epiboly, dorsal view: *fkd3* expression is missing anterior to the diencephalic-mesencephalic boundary in *oep* mutants. (F) *pax6*, 3-somite stage, lateral view: the *pax6* expression domain in the presumptive diencephalon reaches the anterior border of the CNS in *oep* mutants. (G) *pax2*, 12-somite stage, lateral view: *pax2* expression is normal in the otic placode (asterisk) and in the midbrain (arrow) while the expression domain in the optic stalk (triangle) is missing. (H) *dlx3*, 12-somite stage, lateral view: the *dlx3* expression is normal in the otic placode (asterisk) but absent in the olfactory placode (triangle) in *oep* mutants. (J) *shh* and *pax2*, tailbud-stage, view on head region: no *shh* expression can be detected in the brain anterior of the *pax2*-positive midbrain (asterisk). The axial transcripts posterior of the midbrain are located in the notochord. (K) *shh*, 22 hours, lateral view on tail region: *shh* expression is normal in the slightly undulated notochord but absent in the ventral cells of the spinal cord.

trulation, as indicated by the expression of *no tail* (*ntl*; Schulte-Merker et al., 1992; Fig. 2C). At the end of gastrulation, the notochord is slightly shorter, but not broader, and the density of *ntl*-positive cells is increased. No significant difference has been found in the number of *ntl*-positive nuclei in the axis of *oep* and wild-type embryos.

In the neuroectoderm, the earliest differences between *oep* mutants and wild-type siblings have been found at midgastrula stages, about 3 hours after the alterations of the *gsc* expression in the mesendoderm had become apparent. As an early neural marker, we used the forkhead domain gene *fkd3* (J. O., unpublished), which is expressed in presumptive neuroectodermal cells beginning shortly before the onset of gastrulation. While the expression of *fkd3* appears normal at shield stage (not shown) and in the posterior region of the presumptive neuroectoderm at 70% epiboly, the domain anterior of the presumptive diencephalic-mesencephalic boundary is completely absent (Fig. 2E), revealing anterior deficiencies in the neuroectoderm of *oep* mutants. The lack of anterior forebrain structures is also reflected by the expression of other genes at later stages of development: the expression of *pax6* (formerly called *pax[a]*; Krauss et al., 1991) at the 3-somite stage in the presumptive diencephalon reaches the anterior boundary of the head rather than fading out as in wild-type embryos (Fig. 2F), suggesting that brain regions rostral to the diencephalic *pax6* expression domain are missing in *oep* mutants. In addition, the expression of *dlx3* (Akimenko et al., 1994) in the region of the olfactory placodes, which normally overly the telencephalon, is absent in *oep* mutants while it is normally expressed in the more posteriorly derived otic placodes (Fig. 2H).

Other markers reveal defects in the ventral specification of the neuroectoderm throughout the whole length of the axis: the expression of *sonic hedgehog* (*shh*, Krauss et al., 1993) is missing in ventral cells of the brain and the floorplate of the trunk in *oep* mutants (Fig. 2J,K). An additional neuroectodermal defect of *oep* mutants, the fusion of the eyes, is anticipated by the expression of *pax2* (formerly called *pax[b]*; Krauss et al., 1991), which is normally expressed in the optic stalk in proximal regions of the eye primordia. In *oep* mutants, this expression is missing, consistent with the subsequent lack of a separation of the eye field (Fig. 2G).

Altered morphology and gene expression of *dirty nose* mutants

Defects in derivatives of the prechordal plate have also been found in *dirty nose* (*dns*) mutants. Similar to *oep* mutants, *dns* mutant embryos lack the hatching gland and fail to hatch. However, *dns* embryos show no obvious defects during gastrulation. At day 1 of development, brownish looking apoptotic cells, possibly the hatching gland precursors, are found in the anterior region of the head underneath the eyes (Fig. 1G,H). When manually dechorionated, the mutants survive to adulthood.

With molecular markers, alterations in cell specification can already be detected at early gastrula stages, when the expression of *gsc* in dorsal mesodermal cells is slightly reduced in *dns* mutants (Fig. 2B). At the 10-somite stage, before cell death can be detected in this population of cells by acridine orange staining, the staining for Fkd2 protein (R. M. W. and J. O., unpublished) is much weaker in the hatching gland precursors of the prechordal plate, and the stained nuclei appear much smaller than in wild-type siblings (Fig. 2D). The *fkd2*-expressing cells of *dns* mutants stay at the anterior border of the head region rather than spreading onto the yolk sac to form the hatching glands.

Genes required for convergence and extension movements: *spadetail* and *trilobite*

While the main defects in *oep* and possibly *dns* mutants are observed in the anterior region of the developing body axis,

Table 1. Mutations identified in genes required for morphogenesis during gastrulation and tail formation

Gene	Alleles	Phenotypic description	Other references
one-eyed-pinhead	*oep*^{tz257}	No prechordal plate, no hatching gland, fused eyes, no floorplate, reduced heart; reduced cell migration of anterior dorsal mesendoderm	a,b,c
dirty nose	*dns*^{te350}	Cell death in prechordal plate, no hatching glands; viable when dechorionated	
zwangsjacke	*zja*^{ta65}	Delayed hatching; viable	
spadetail	*spt*^{tm41} *spt*^{tq5}	Enlarged tailbud, no trunk somites; reduced dorsal convergence	d
biber	*bib*^{tb8}	Strongly compressed body axis, indistinct somites, posterior trunk and tail broader	
trilobite	*tri*^{tc240} *tri*^{tk50}	Short body axis, notochord and somites broader; reduced convergent extension	e
pipetail	*ppt*^{ta98} *ppt*^{tc271} *ppt*^{te1} *ppt*^{ti265} *ppt*^{th278}	Short body axis, undulated notochord, posterior somites broader; reduced ventral movement of the tailbud along the yolk sac; tip of the tail does not detach from the yolk extension	f
kugelig	*kgg*^{tl240} *kgg*^{tv205}	Short body axis, no formation of yolk extension	
samson	*sam*^{tb233}	Short body axis; thinner notochord and wider somites	
ugly duckling	*udu*^{tu24}	Short body axis, cell death in neuroectoderm at day 1, fewer blood cells; no pattern defects detectable with molecular markers	
indigested	*ind*^{ti228}	Remnants of yolk exhibit brown color; viable; homozygous adults appear normal and are fertile	
malprofit	*mpt*^{ts92}	Remnants of yolk exhibit brown color; viable; homozygous adults are smaller	

References: a, Heisenberg et al. (1996); b, Brand et al. (1996); c, Schier et al. (1996); d, Kimmel et al. (1989); e, Solnica-Krezel et al. (1996); f, Piotrowski et al. (1996).

spadetail (*spt*) and *trilobite* (*tri*) mutants display alterations over the entire length of the axis. Two new alleles of the previously identified gene *spt* (Kimmel et al., 1989) have been isolated, spt^{tm41} and spt^{tq5}, both of which are of similar strength to the previously known allele spt^{b104}. In *spt* mutant embryos, no somites are formed in the trunk, while the notochord appears rather normal (Fig. 3A, see below). The tailbud is greatly enlarged (Fig. 3B).

Two alleles of *tri* have been isolated, tri^{tk50} and tri^{tc240}, with tri^{tk50} causing a clearly stronger phenotype than tri^{tc240} (see also Solnica-Krezel et al., 1996). In contrast to *spt* mutants, *tri* mutant embryos have trunk somites. Compared to wild-type siblings, the somites are more compressed in the anteroposterior axis and broader in the mediolateral axis, as already apparent at the 2-somite stage. The notochord is also shorter and slightly broader (Fig. 3A). Although the length of the body axis is reduced, the broader notochord shows little indication of undulation compared to other short mutants like *pipetail* (see below).

The morphological alterations in the axis of *spt* and *tri* mutant embryos suggest that convergent extension movements at the ventrolateral and the dorsal side, respectively, are affected. This is supported by the altered expression pattern of marker genes. At the 80% epiboly stage, the lack of dorsal convergent movements of the ventrolaterally derived mesoderm in *spt* mutant embryos is revealed by the expression pattern of *sna1* (Hammerschmidt and Nüsslein-Volhard, 1993; Thisse et al., 1993), which stays restricted to ventrolateral marginal regions rather than forming two paraxial stripes (Fig. 4A). At the 4-somite stage, the expression of *myoD* (Weinberg et al., 1996) in two adaxial lines adjacent to the notochord is strongly reduced (Fig. 4C), and the expression in more lateral regions, corresponding to the positions where the somites are normally formed in the wild-type siblings, is completely missing. These paraxial deficiencies have been shown to be caused by a failure of muscle precursor cells to converge to the dorsal axis (Ho and Kane, 1990). Instead, these cells remain in ventrolateral positions and eventually end up in the tailbud, which is much thicker and contains many more cells in the posterior region of *spt* mutants at early somite stages, as revealed by the expression of *eve1* (Fig. 4D; Joly et al., 1993).

The axial mesoderm is only slightly affected in *spt* mutants. The *ntl* expression domain is slightly broader than in wild-type siblings at early somite stages (Fig. 4B, see also Fig. 4C for the increased distance between the *myoD*-positive adaxial stripes). These observations suggest that the defects in gastrulating *spt* mutant embryos are largely restricted to the dorsal convergence movements of ventrolateral cells towards the dorsal axis.

In contrast, embryos homozygous for the strong tri^{tk50} allele exhibit only a subtle difference in the expression pattern of *sna1* in ventrolateral positions at 70% epiboly (Fig. 4E). In the dorsal midline, however, alterations can be detected at the end of gastrulation. As revealed by the expression pattern of *ntl*, the presumptive notochord is considerably broader and shorter, although no significant difference in the number of *ntl*-positive cells has been found (Fig. 4F). As revealed by the expression of *myoD*, the paraxial mesoderm of tri^{tk50}/tri^{tk50} embryos has about 60% of its normal length (Fig. 4G). The *eve1* expression domain in the tailbud of *tri* mutant embryos, although about twice as broad as in wild type, appears to contain the normal number of cells (Fig. 4H). These observations suggest that in *tri* mutants, in contrast to *spt* mutants, ventrolateral cells converge normally towards the axis, but convergent extension movements in the axis itself are reduced.

Genes required for tail formation: *pipetail* and *kugelig*

Seven short mutants defining two complementation groups were isolated which show an impaired outgrowth of the tail.

Five alleles of *pipetail* (*ppt*) were isolated, ppt^{ta98}, ppt^{te1}, ppt^{tc271}, ppt^{ti265} and ppt^{th278}, which all are of similar strength. *ppt* mutant embryos can be morphologically identified at the 2-somite stage, when their body axis is shorter, spanning an angle of about 270° instead of about 300° as in wild-type siblings (see Fig. 5A for 8-somite stage). Normally, the tailbud moves ventrally after the end of gastrulation. This movement seems to be blocked in *ppt* mutants, leaving the tailbud closer to the point of germ ring closure. The whole body axis becomes compressed: the notochord is undulated (Fig. 5B) and the somites are thinner along the anteroposterior axis (Fig. 5A,B). The formation of the yolk tube starts normally, although the yolk tube is about twice as thick and half as long as in wild-type embryos at the 24-somite stage. The region posterior to the yolk tube is several times shorter than in wild-type siblings and remains attached to the yolk tube much longer than in wild-type siblings (Fig. 5C). At day 5 of development, the *ppt* mutant larvae have only about 80% of the normal length. Although the notochord and the neurocoel are bent at the tip of the tail (Fig. 5E), the gap of the ventral melanophore stripe is present, indicating that despite the compression posterior structures are properly patterned.

In addition to the defects in the tail, *ppt* mutants display an impaired growth of the head skeleton. In wild-type larvae, cartilaginous elements of the neurocranium and the pharyngeal skeleton extend anteriorly beyond the eyes at days 4 and 5 of development. In *ppt* mutants, however, these elements show a reduction in length and abnormal cartilage differentiation, features shared by the 'hammerhead' class of mutants (Fig. 5D, Piotrowski et al., 1996).

Two alleles of *kugelig* (*kgg*) were isolated. The *kgg* phenotype becomes obvious at the 14-somite stage. In contrast to *ppt* mutants, the ventral migration of the tailbud on the yolk sac occurs normally in *kgg* mutants. However, the constriction of the posterior part of the yolk sac and the subsequent formation of the yolk tube are blocked. The yolk tube of *kgg* mutants has at most 10% of the normal length, leading to a rather spherical ('kugelig' in German) body shape (Fig. 5C). The region posterior to the yolk tube is only slightly shorter than in wild-type embryos. During subsequent development, the posterior part of the tail often curls up and folds back in a rather sharp angle. In contrast to *ppt* mutants, notochord and neurocoel end normally in the tail tip of *kgg* mutant embryos. In the trunk, however, the neurocoel seems slightly enlarged and disrupted at variable positions. Although not fully understood yet, these neurocoel defects might be secondary consequences of the curled shape of the trunk.

Altered gene expression in *ppt* and *kgg* mutants

In situ analysis of *ppt* mutants was carried out with markers specific for different regions of the tailbud and the tail. In early somite stages, *eve1* (Fig. 5L), *ntl* (Fig. 5H) and *sna1* (not shown),

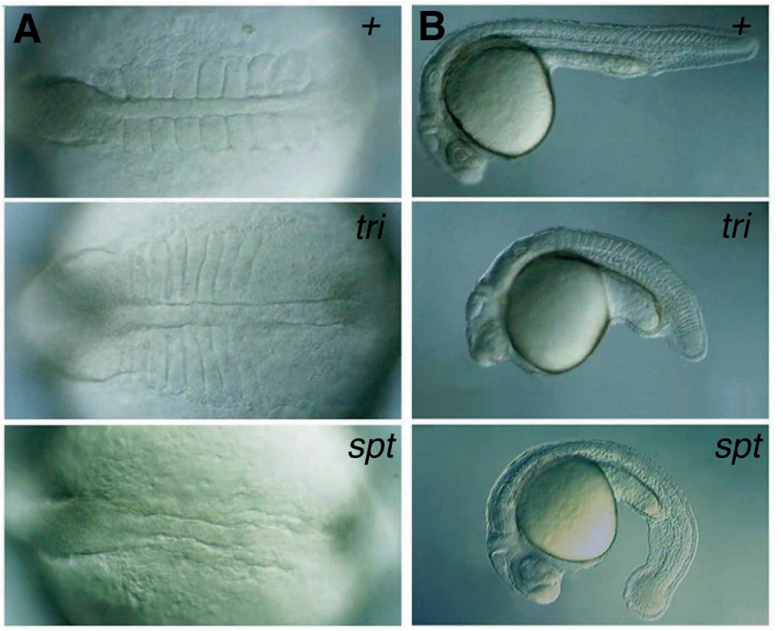

Fig. 3. Alterations in morphology in *trilobite* (*tri*^{tk50}) and *spadetail* (*spt*^{b104}) mutants, compared to wild type (+). (A) 8-somite stage, dorsal view: both notochord and somites are shorter and wider in *tri* mutants. No somites are formed in *spt* mutants. (B) 30 hours, lateral view: *tri* embryos are shorter than wild-type and *spt* mutant embryos. Note the accumulation of cells at the tip of the tail in *spt* mutants.

all of which are expressed in presumptive mesodermal cells of the tailbud, show a normal expression pattern, suggesting that the formation of the posterior mesoderm is normal. The same applies to genes expressed in posterior neuroectoderm like *pou2* (Takeda et al., 1994) and *cad1* (Joly et al., 1992) (not shown). The expression of *wnt[a]*, a zebrafish *wnt* gene with highest structural similarity to the mouse genes *wnt3* and *wnt3a* (Krauss et al., 1992), although of normal intensity, reflects the impaired ventral growth of the tailbud described above. While in a wild-type embryo of the 5-somite stage the expression domain acquires the shape of a full semicircle, the expression domain in the mutant is still round with a small circular gap in the middle

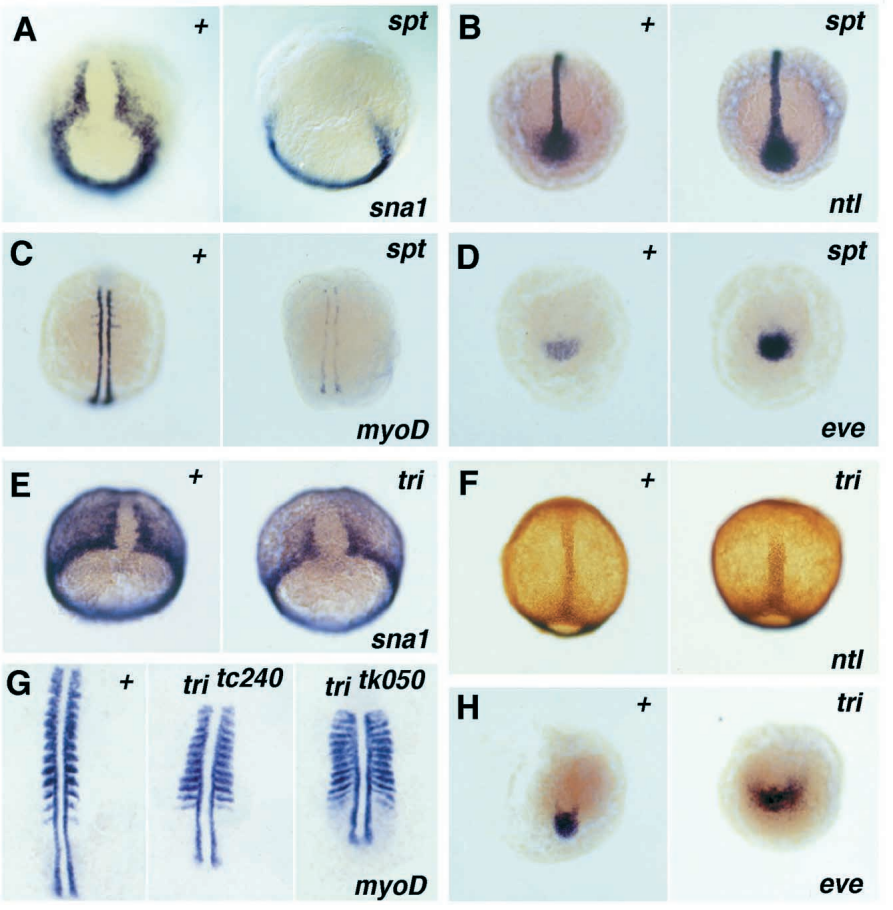

Fig. 4. Altered gene expression in the mesoderm of *spadetail* (*spt*^{b104}) and *trilobite* (*tri*^{tk50}) mutants compared to wild type (+), detected by in situ hybridization (A-E,G,H) and immunostaining (F). (A) *sna1*, 80% epiboly, dorsovegetal view. (B) *ntl*, 4-somite stage, dorsovegetal view. (C) *myoD*, 4-somite stage, dorsal view. (D) *eve1*, 4-somite stage, vegetal view. (E) *sna1*, 70% epiboly, dorsovegetal view. (F) *ntl*, 95% epiboly, dorsal view. (G) *myoD*, 10-somite stage, dorsal view on spread embryos, anterior on top. (H) *eve1*, 10-somite stage, vegetal view.

(Fig. 5G), showing that the tailbud has maintained the same conformation as at the end of gastrulation. Only one of all tested marker genes shows a significant reduction in the level of expression from early somite stages on: *wnt[b]*, a zebrafish *wnt* gene with highest structural similarity to the mouse genes *wnt5a* and *wnt5b* (Krauss et al., 1992). Its expression is strongly reduced in the whole posterior region, including the posterior-most somites (Fig. 5F). At the 28-somite stage, the impaired outgrowth of the region posterior to the yolk tube is reflected by the *eve1* expression. In addition to the presumptive mesodermal cells at the tip of the tail, *eve1* is expressed in a line of distal cells that spans, ventrally and dorsally, from the anus to the tail tip (Fig. 5L). In the mutant, this distal expression domain does not extend. Rather, it is broader than in wild-type siblings and remains at its original position close to the posterior end of the yolk tube, while inner regions of the tail attempt to extend normally (Fig. 5L, see also Fig. 5C).

The trunk phenotype is reflected by the expression pattern of *ntl* and *myoD*. The *ntl* expression domain in the notochord is undulated (Fig. 5H), as are the *myoD*-positive adaxial lines (Fig. 5J). The somitic *myoD* expression pattern is more compressed in the anteroposterior axis, and the expression in the posterior somites is broader, extending to more lateral positions (Fig. 5J).

In contrast to *ppt* mutants, posterior somites in *kgg* mutants are compressed without showing a lateral expansion (Fig. 5K). Since *kgg* mutants show an impaired formation of the yolk tube, we especially investigated the expression pattern of genes expressed in the region of the presumptive anus and just anterior to it, such as *dlx3* (Akimenko et al., 1994) and *cad1* (Joly et al., 1992). However, none of these genes shows an altered expression before the phenotype becomes morphologically visible (not shown).

DISCUSSION

We have identified several genes required for the various morphogenetic movements that occur during zebrafish gastrulation and tail formation. Mutants in *one-eyed-pinhead* (*oep*) and *dirty nose* (*dns*) display defects in prechordal plate formation. Mutants in *spadetail* (*spt*) and *trilobite* (*tri*) display alterations in different aspects of dorsal convergent extension movements, while in *pipetail* (*ppt*) and *kugelig* (*kgg*) mutants morpho-

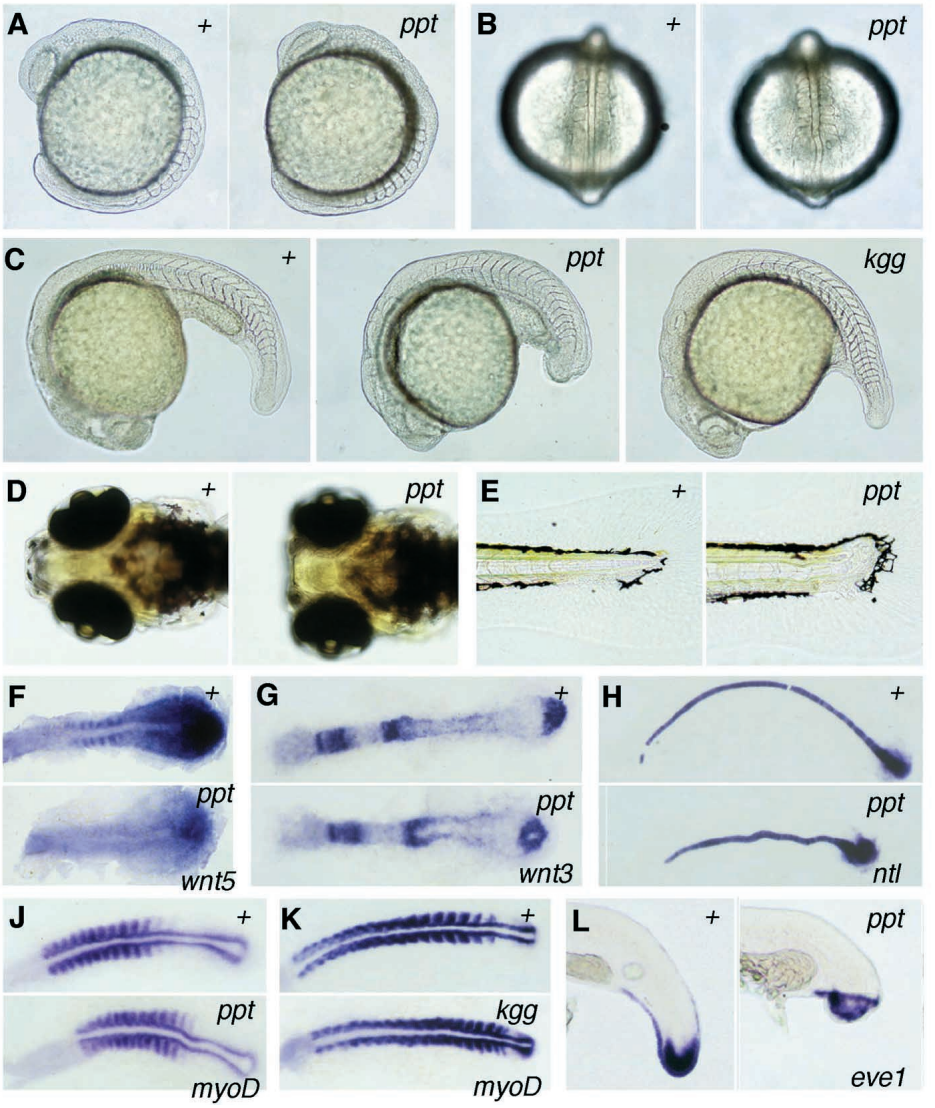

Fig. 5. Alterations in morphology and gene expression of *pipetail* (*ppt*^{ta98}, A-J,L) and *kugelig* (*kgg*^{tl240}, C,K) mutant embryos, compared to wild type (+). (A) 10-somite stage, lateral view. (B) 10-somite stage, dorsal view: in *ppt* mutants, the notochord is undulated and the somites are condensed along the anteroposterior axis. Somites 9 and 10 and the presomitic mesoderm show a slight lateral expansion. (C) 24-somite stage, lateral view. (D) Day 5, ventral view of head: the head skeleton forms but fails to extend beyond the eyes, leading to a slight broadening of the head in *ppt* mutants. (E) Day 5, lateral view of tip of tail: the notochord and the neurocoel are slightly kinked at the end of the tail; the ventral gap of the melanophore stripe is present. (F-K) Dorsal view on spread embryo, anterior left: (F) *wnt5*, 5-somite stage: the expression of *wnt5* is significantly reduced in somites and tailbud of *ppt* mutants. (G) *wnt3*, 5-somite stage. (H) *ntl*, 8-somite stage. (J) *myoD*, 12-somite stage: all somites are condensed, the posterior somites are laterally expanded in *ppt* mutants. (K) *myoD*, 16-somite stage: the posterior somites are condensed but not laterally expanded in *kgg* mutants. (L) *eve1*, 28-somite stage, lateral view on tail.

genetic processes specific to tail formation are affected. Mutations in additional genes required for a normal extension of the body axis are described in Table 1. No mutants lacking involution were isolated, while four mutants affecting epiboly movements have been found (Kane et al., 1996).

oep affects several developmental processes

one-eyed-pinhead (*oep*) mutants show four main defects: a lack of the anteriormost structures in both the mesoderm and the neuroectoderm, a fusion of the eyes, and a lack of ventral specification in the central nervous system over the entire length of the body axis. With molecular markers, alterations first become visible in the presumptive prechordal plate of the mesoderm, starting before the onset of gastrulation. The defects in the neuroectoderm appear later during gastrulation and somitogenesis. The temporal development of the different phenotypic traits suggests that the alterations in the neuroectoderm might be a consequence of the defects in the prechordal plate. This notion is supported by findings that in normal vertebrate development, the separation of the eye field depends on vertical signals emanating from the underlying axial head mesendoderm (Brun, 1981). Interestingly, the ventralization of the neural tube is blocked over the entire length of the body axis, although in the posterior regions of the axis, no structural defects have been found in the underlying mesoderm, the notochord. This observation might suggest that the ventral specification of the neuroectoderm takes place at early stages of gastrulation (60% epiboly), when the *goosecoid*-positive presumptive prechordal plate cells underlie the not-yet-extended neuroectoderm over its entire anteroposterior length.

In wild-type zebrafish embryos, the prechordal cells are known to be very motile (R. M. W. and D. A. K., unpublished results) and are supposed to display active cell migration, as it has been demonstrated for prechordal cells in *Xenopus* (Winkelbaur, 1990; Winkelbaur and Selchow, 1992). The altered shape of the residual *gsc* expression domain in some *oep* mutants suggests that *oep* is required for a proper rostral movement of cells at the anterior edge of the hypoblast. The coincidence of the lack of *gsc* expression and the lack of these anterior movements in *oep* mutants is consistent with the finding that ectopic *gsc* can initiate cell migration movements in *Xenopus* embryos (Niehrs et al., 1993).

These anterior movements appear to be necessary for the normal extension of the body axis, as the body axis is compressed in *oep* mutants at late gastrula stages and the notochord is slightly undulated in older embryos. A similar compression of the body axis is observed in other mutants with defects in the prechordal plate (*cyclops*, Brand et al., 1996; *silberblick*, Heisenberg et al., 1996), and in mutants with defects in the axis itself (*trilobite*, see below) or at its posterior end (*pipetail*, see below). Altogether, the phenotypes of the various mutants suggest that the extension of the body axis is driven by different forces: an anterior movement of prechordal cells at the anterior edge of the hypoblast, a posterior movement of the tailbud at the posterior end of the axis, and extension within the axis driven by medial intercalation.

spadetail and *trilobite* are required for different aspects of convergent extension movements

While *oep*, *cyc*, *slb* and *ppt* appear to be involved in movements of anterior and posterior cells at the leading edges of the axis, *spadetail* (*spt*) and *trilobite* (*tri*) are required for convergent extension movements of cells between these edges. As previously described, *spt* mutant embryos display defects in the movement of ventrolateral cells to the dorsal midline. The extension movements in the midline, however, appear rather normal at gastrula and early somite stages. In contrast to *spt*, *tri* mutant embryos exhibit normal convergent movements of ventrolateral cells to the dorsal side, while the convergent extension in the axis is strongly impaired. Convergent extension movements have been shown to be driven by mediolateral cell intercalations (Warga and Kimmel, 1990). The phenotypes of *spt* and *tri* mutants, however, indicate that convergent extension movements in ventrolateral regions towards the axis and on the dorsal side of the embryo along the length of the axis can be uncoupled from one another.

pipetail and *kugelig* are required for distinct processes during tail formation

Previous studies have revealed that the formation of the tail is a continuation of gastrulation and depends on genes already required during gastrulation (Gont et al., 1993; Tucker and Slack, 1995). Much of the material of the tail is formed in the tailbud and later in the tip of the tail, where a 'mini-gastrulation' takes place. *pipetail* (*ppt*) and *kugelig* (*kgg*) mutants, however, show specific defects during tail formation, although gastrulation and formation of tail material in the tailbud and the tip of the tail appear largely normal. This suggests that the genes regulate processes that occur in addition to the continued gastrulation processes in order to allow a normal outgrowth of the tail. Alternatively, the effects of the mutations during gastrulation might be very subtle or compensated by maternally supplied gene products. In *ppt* mutant embryos, the tailbud fails to move more ventrally on the yolk sac after closure of the germ ring. Later, the detachment of the tip of the tail from the yolk is impaired. Of all posterior marker genes tested, only *wnt5* shows a significantly reduced expression in the posterior region of *ppt* mutants from early developmental stages on, suggesting that *ppt* might be zebrafish *wnt5* or a gene involved in the activation of the *wnt5* expression. We are currently testing whether the mutation in *ppt* is physically linked to the *wnt5* gene.

In contrast to *ppt* mutant embryos, *kgg* mutants exhibit a normal ventral movement of the tailbud after closure of the germ ring and a rather normal detachment of the forming tail from the yolk. However, the formation of the yolk tube is strongly impaired, which leads to a compression of the posterior part of the body axis.

The mutants described above display specific and unique effects on different morphogenetic processes of early zebrafish development. We expect them to be valuable tools for the investigation of the various morphogenetic processes that occur during gastrulation and tail formation.

M. H. and F. P. contributed equally to this work. We are very grateful to Dr Andrew McMahon, in whose laboratory much of the mutant analysis has been carried out. Additionally, we would like to thank Ed Sullivan for his help and advice during the setting-up of a fish facility in the McMahon laboratory. Dr Eric Weinberg generously supplied us with the *myoD* cDNA prior to publication. Published reagents were obtained from Drs Marie-Andrée Akimenko, Jean-Stéphane Joly, Stefan Krauss and Stefan Schulte-Merker.

REFERENCES

Akimenko, M.-A., Ekker, M., Wegner, J., Lin, W. and Westerfield, M. (1994). Combinatorial expression of three zebrafish genes related to *distal-less*: part of a homeobox gene code for the head. *J. Neurosci.* **16**, 3475-3486.

Brand, M., Heisenberg, C.-P., Warga, R., Pelegri, F., Karlstrom, R. O., Beuchle, D., Picker, A., Jiang, Y.-J., Furutani-Seiki, M., van Eeden, F. J. M., Granato, M., Haffter, P., Hammerschmidt, M., Kane, D., Kelsh, R., Mullins, M., Odenthal, J. and Nüsslein-Volhard, C. (1996). Mutations affecting development of the midline and general body shape during zebrafish embryogenesis. *Development* **123**, 129-142.

Brun, R. B. (1981). The movement of the prospective eye vesicles from the neural plate into the neural fold in *Ambystoma mexicanum* and *Xenopus laevis*. *Dev. Biol.* **88**, 192-199.

Gont, L. K., Steinbeisser, H., Blumberg, B. and De Robertis, E. M. (1993). Tail formation as a continuation of gastrulation: the multiple cell populations of the Xenopus tailbud derive from the late blastopore lip. *Development* **119**, 991-1004.

Hammerschmidt, M. and Nüsslein-Volhard, C. (1993). The expression of a zebrafish gene homologous to *Drosophila snail* suggests a conserved function in invertebrate and vertebrate gastrulation. *Development* **119**, 1107-1118.

Hammerschmidt, M., Pelegri, F., Mullins, M. C., Kane, D. A., van Eeden, F. J. M., Granato, M., Brand, M., Furutani-Seiki, M., Haffter, P., Heisenberg, C.-P., Jiang, Y.-J., Kelsh, R. N., Odenthal, J., Warga, R. M. and Nüsslein-Volhard, C. (1996). *dino* and *mercedes*, two genes regulating dorsal development in the zebrafish embryo. *Development* **123**, 95-102.

Hatta, K., Kimmel, C. B., Ho, R. K. and Walker, C. (1991). The *cyclops* mutation blocks specification of the floor plate of the zebrafish central nervous system. *Nature* **350**, 339-341.

Heisenberg, C.-P., Brand, M., Jiang, Y.-J., Warga, R. M., Beuchle, D., van Eeden, F. J. M., Furutani-Seiki, M., Granato, M., Haffter, P., Hammerschmidt, M., Kane, D. A., Kelsh, R. N., Mullins, M. C., Odenthal, J. and Nüsslein-Volhard, C. (1996). Genes involved in forebrain development in the zebrafish, *Danio rerio*. *Development* **123**, 191-203.

Ho, R. K. and Kane, D. A. (1990). Cell-autonomous action of zebrafish *spt-1* mutation in specific mesodermal precursors. *Nature* **348**, 728-730.

Joly, J.-S., Joly, C., Schulte-Merker, S., Boulkebache, H. and Condamine, H. (1993). The ventral and posterior expression of the homeobox gene *eve1* is perturbed in dorsalized and mutant embryos. *Development* **119**, 1261-1275.

Joly, J.-S., Maury, M., Joly, C., Duprey, P., Boulkebache, H. and Condamine, H. (1992). Expression of a zebrafish *caudal* homeobox gene correlates with the establishment of posterior lineages at gastrulation. *Differentiation* **50**, 75-87.

Kane, D. A., Hammerschmidt, M., Mullins, M. C., Maischein, H.-M., Brand, M., van Eeden, F. J. M., Furutani-Seiki, M., Granato, M., Haffter, P., Heisenberg, C.-P., Jiang, Y.-J., Kelsh, R. N., Odenthal, J., Warga, R. M. and Nüsslein-Volhard, C. (1996). The zebrafish epiboly mutants. *Development* **123**, 47-55.

Kimmel, C. B., Kane, D. A., Walker, C., Warga, R. M. and Rothman, M. B. (1989). A mutation that changes cell movement and cell fate in the zebrafish embryo. *Nature* **337**, 358-362.

Kimmel, C. B., Ballard, W. W., Kimmel, S. R., Ullmann, B. and Schilling, T. F. (1995). Stages of embryonic development of the zebrafish. *Dev. Dyn.* **203**, 253-310.

Krauss, S., Concordet, J.-P. and Ingham, P. W. (1993). A functionally conserved homolog of the *Drosophila* segment polarity gene *hh* is expressed in tissues with polarizing activity in zebrafish embryos. *Cell* **75**, 1431-1444.

Krauss, S., Johansen, T., Korzh, V. and Fjose, A. (1991). Expression pattern of zebrafish *pax* genes suggests a role in early brain regionalization. *Nature* **353**, 267-270.

Krauss, S., Korzh, V., Fjose, A. and Johansen, T. (1992). Expression of four zebrafish *wnt*-related genes during embryogenesis. *Development* **115**, 249-259.

Mullins, M. C., Hammerschmidt, M., Haffter, P. and Nüsslein-Volhard, C. (1994). Large-scale mutagenesis in the zebrafish: in search of genes controlling development in a vertebrate. *Curr. Biol.* **4**, 189-202.

Mullins, M. C., Hammerschmidt, M., Kane, D. A., Odenthal, J., Brand, M., van Eeden, F. J. M., Furutani-Seiki, M., Granato, M., Haffter, P., Heisenberg, C.-P., Jiang, Y.-J., Kelsh, R. N. and Nüsslein-Volhard, C. (1996). Genes establishing dorsoventral pattern formation in the zebrafish embryo: the ventral specifying genes. *Development* **123**, 81-93.

Niehrs, C., Keller, R., Cho, K. W. Y. and De Robertis, E. M. (1993). The homeobox gene *goosecoid* controls cell migration in *Xenopus* embryos. *Cell* **72**, 491-503.

Piotrowski, T., Schilling, T. F., Brand, M., Jiang, Y.-J., Heisenberg, C.-P., Beuchle, D., Grandel, H., van Eeden, F. J. M., Furutani-Seiki, M., Granato, M., Haffter, P., Hammerschmidt, M., Kane, D. A., Kelsh, R. N., Mullins, M. C., Odenthal, J., Warga, R. M. and Nüsslein-Volhard, C. (1996). Jaw and branchial arch mutants in zebrafish II: anterior arches and cartilage differentiation. *Development* **123**, 345-356.

Schier, A. F., Neuhauss, S. C. F., Harvey, M., Malicki, J., Solnica-Krezel, L., Stainier, D. Y. R., Zwartkruis, F., Abdelilah, S., Stemple, D. L., Rangini, Z., Yang, H. and Driever, W. (1996). Mutations affecting the development of the embryonic zebrafish brain. *Development* **123**, 165-178.

Schulte-Merker, S., Ho, R. K., Herrmann, B. G. and Nüsslein-Volhard, C. (1992). The protein product of the zebrafish homologue of the mouse *T* gene is expressed in nuclei of the germ ring and the notochord of the early embryo. *Development* **116**, 1021-1032.

Schulte-Merker, S., Hammerschmidt, M., Beuchle, D., Cho, K. W., DeRobertis, E. M. and Nüsslein-Volhard, C. (1994). Expression of the zebrafish *goosecoid* and *no tail* gene products in wild-type and mutant *ntl* embryo. *Development* **120**, 843-852.

Smith, J. C. and Howard, J. E. (1992). Mesoderm-inducing factors and the control of gastrulation. *Development* **Supplement**, 127-136.

Solnica-Krezel, L., Stemple, D. L., Mountcastle-Shah, E., Rangini, Z., Neuhauss, S. C. F., Malicki, J., Schier, A. F., Stainier, D. Y. R., Zwartkruis, F., Abdelilah, S. and Driever, W. (1996). Mutations affecting cell fates and cellular rearrangements during gastrulation in zebrafish. *Development* **123**, 67-80.

Stachel, S. E., Grunwald, D. J. and Myers, P. Z. (1993). Lithium perturbation and *goosecoid* expression identify a dorsal specification pathway in the pregastrula zebrafish. *Development* **117**, 1261-1274.

Takeda, H., Matsuzaki, T., Oki, T., Miyagawa, T. and Amanuma, H. (1994). A novel POU domain gene, zebrafish *pou2*: expression and roles of two alternatively spliced twin products in early development. *Genes Dev.* **8**, 45-59.

Thisse, C., Thisse, B., Halpern, M. E. and Postlethwait, J. H. (1994). *goosecoid* expression in neuroectoderm and mesendoderm is disrupted in zebrafish *cyclops* gastrulas. *Dev. Biol.* **164**, 420-429.

Thisse, C., Thisse, B., Schilling, T. F. and Postlethwait, J. H. (1993). Structure of the zebrafish *snail1* gene and its expression in wild-type, *spadetail* and *no tail* mutant embryos. *Development* **119**, 1203-1215.

Tucker, A. S. and Slack, J. M. W. (1995). The *Xenopus laevis* tail-forming region. *Development* **121**, 249-262.

Warga, R. M. and Kimmel, C. B. (1990). Cell movements during epiboly and gastrulation in zebrafish. *Development* **108**, 569-80.

Weinberg, E. S., Allende, L. M., Kelly, C. S., Abdelhamid, A., Murakami, T., Andermann, P., Doerre, O. G., Grunwald, D. J. and Riggleman, B. (1996). Developmental regulation of zebrafish *myoD* in wild-type, *no tail* and *spadetail* embryos. *Development* **122**, 271-280.

Westerfield, M. (1994). *The Zebrafish Book*. Eugene, Oregon, University of Oregon Press.

Winkelbaur, R. (1990). Mesoderm cell migration during *Xenopus* gastrulation. *Dev. Biol.* **142**, 155-168.

Winkelbaur, R. and Selchow, A. (1992). Motile behaviour and protrusive activity of migratory mesoderm cells form *Xenopus* gastrula. *Dev. Biol.* **150**, 335-351.

(Accepted 16 April 1996)